Supporting Information

Pairing *Bacteroides vulgatus* LPS structure with its immunomodulatory effects on human cellular models

Flaviana Di Lorenzo,[*†,‡] Molly D. Pither,[†] Michela Martufi,[□] Ilaria Scarinci,[□] Joan Guzman Caldentey,[§] Ewelina Łakomiec,[ϭ] Wojciech Jachymek,[ϭ] Sven C.M. Bruijns,[∞] Sonsoles Martín Santamaría,[§] Julia-Stephanie Frick,[↓] Yvette van Kooyk,[∞] Fabrizio Chiodo,[∞] Alba Silipo,[†,‡] Maria Lina Bernardini,[□] Antonio Molinaro[*†,‡]

[†]Department of Chemical Sciences, University of Naples Federico II, 80126 Naples, Italy

[‡]Task Force on Microbiome Studies, University of Naples Federico II, 80126 Naples, Italy

[□]Department of Biology and Biotechnologies "C. Darwin", Sapienza-University of Rome, 00185 Rome, Italy

[§]Department of Structural and Chemical Biology, Centro de Investigaciones Biológicas, CIB-CSIC, 28040 Madrid, Spain

[ϭ]Hirszfeld Institute of Immunology and Experimental Therapy, Polish Academy of Sciences, Wrocław 53-114, Poland

[∞]Department of Molecular Cell Biology and Immunology, Amsterdam Infection & Immunity Institute and Cancer Center Amsterdam, Amsterdam UMC, Vrije Universiteit Amsterdam, Amsterdam, The Netherlands.

[↓]Institute of Medical Microbiology and Hygiene, University of Tübingen, 72076 Tübingen, Germany

Supporting Tables Section

Table S1. Interpretation of ESI-IT mass spectra of the saccharide domain of the LPS_{Bv}

Oligosaccharide composition	**Mass of the observed ion**	**Calculated mass of the ion**	**Monoisotopic mass of oligosaccharides (Da)**	
	(*m/z*)	(*m/z*)	observed	calculated
Kdo·$HexN_2$·Hex_2·$DeoxyHex_2$·P	627.3	627.19	1256.6	1256.39
Kdo·HexN·Hex_3·$DeoxyHex_2$·P	627.8	627.69	1257.6	1257.38
Kdo·$HexN_2$·Hex_2·$DeoxyHex_2$·P_2	444.6 (-3) 667.3 (-2)	444.45 (-3) 667.18 (-2)	1336.6 1336.8	1336.36
Kdo·$HexN_2$·Hex_2·$DeoxyHex_2$·P_2	678.3#	-	1336.6	1336.36
Kdo·$HexN_2$·Hex_3·$DeoxyHex_2$·P_2	748.3	748.20	1498.6	1498.41
Kdo·$HexN_2$·Hex_3·$DeoxyHex_3$·P_1	781.4	781.25	1564.8	1564.50
Kdo·$HexN_3$·Hex_3·$DeoxyHex_2$·P_1	788.8	788.76	1579.6	1579.52
Kdo·$HexN_2$·Hex_3·$DeoxyHex_3$·P_2	821.3	821.23	1644.6	1644.47
Kdo·$HexN_3$·Hex_3·$DeoxyHex_2$·P_2	828.8	828.74	1659.6	1659.48
Kdo·$HexN_2$·Hex_4·$DeoxyHex_4$·P_2	650.0 (-3) 975.4 (-2)	649.86 (-3) 975.29 (-2)	1953.0 1952.8	1952.58
Kdo·$HexN_2$·Hex_5·$DeoxyHex_5$·P_2	1129.4	1129.34	2260.8	2260.69

# indicates $[M-3H+Na]^{2-}$ ion.

Supporting Figures Section

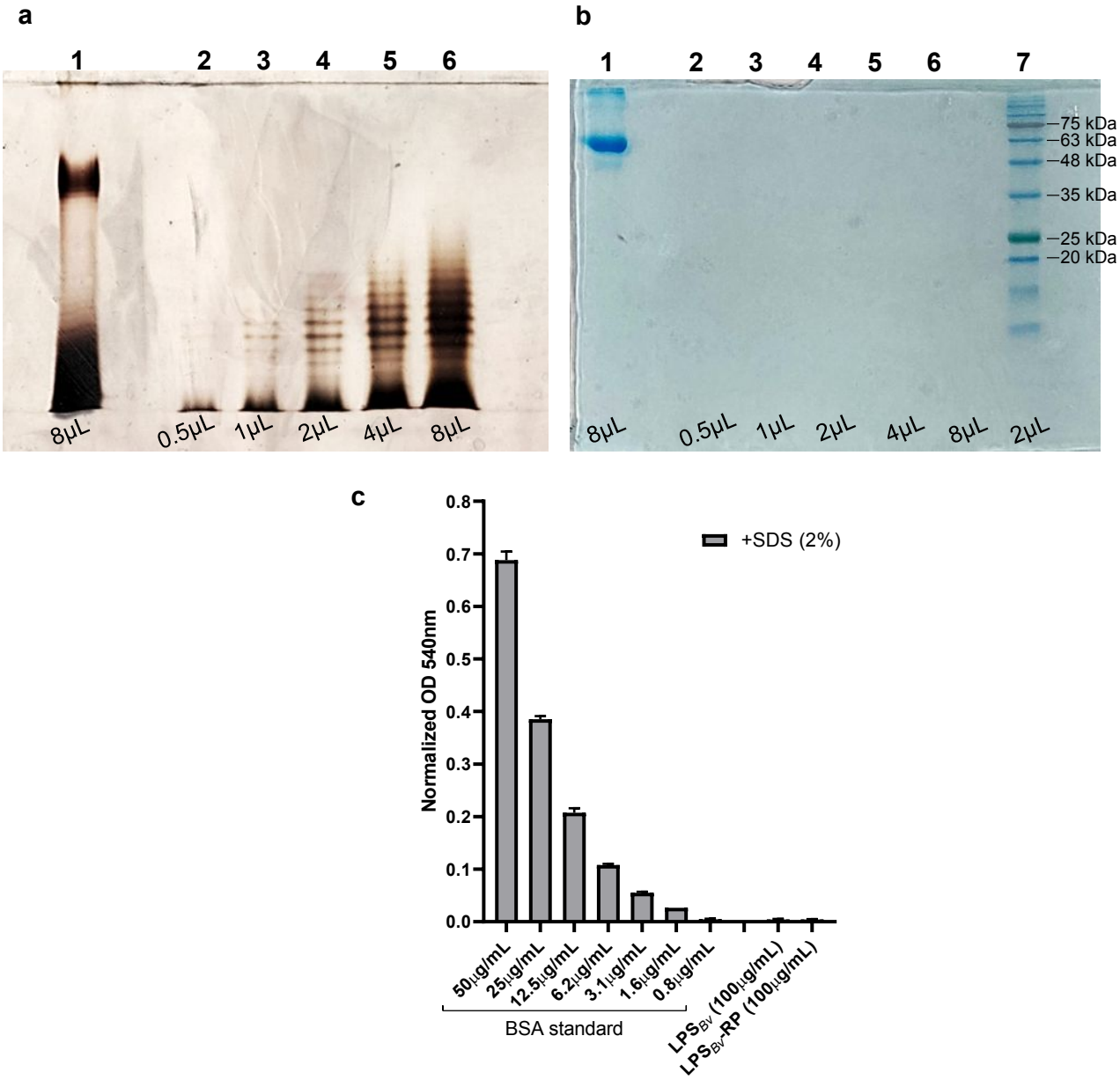

Figure S1. Silver (**a**) and Coomassie Brilliant Blue (**b**) staining of SDS-PAGE of LPS_{Bv}. In the silver stained SDS-PAGE gel (**a**) LPS from *E. coli* O127:B8 (8 µL) (Lane 1) was used as a benchmark; 0.5 µL (Lane 2), 1 µL (Lane 3), 2 µL (Lane 4), 4 µL (Lane 5) and 8 µL (Lane 6) of 1 mg/mL solution of LPS_{Bv} were loaded on the gel. In the Coomassie Brilliant Blue stained SDS-PAGE gel (**b**) bovine serum albumin (BSA) (8 µL) (Lane 1) and BLUeye Prestained Protein Ladder (2 µL) (Lane 7) were used as references. Once again 0.5 µL (Lane 2), 1 µL (Lane 3), 2 µL (Lane 4), 4 µL (Lane 5) and 8 µL (Lane 6) of 1 mg/mL solution of LPS_{Bv} were loaded on the gel. (**c**) Micro BCA™ Protein Assay executed in duplicate in presence of 2 % SDS. BSA at several concentrations has been used as standard. The graph shows the normalized optical density (OD) over the background signal from water samples.

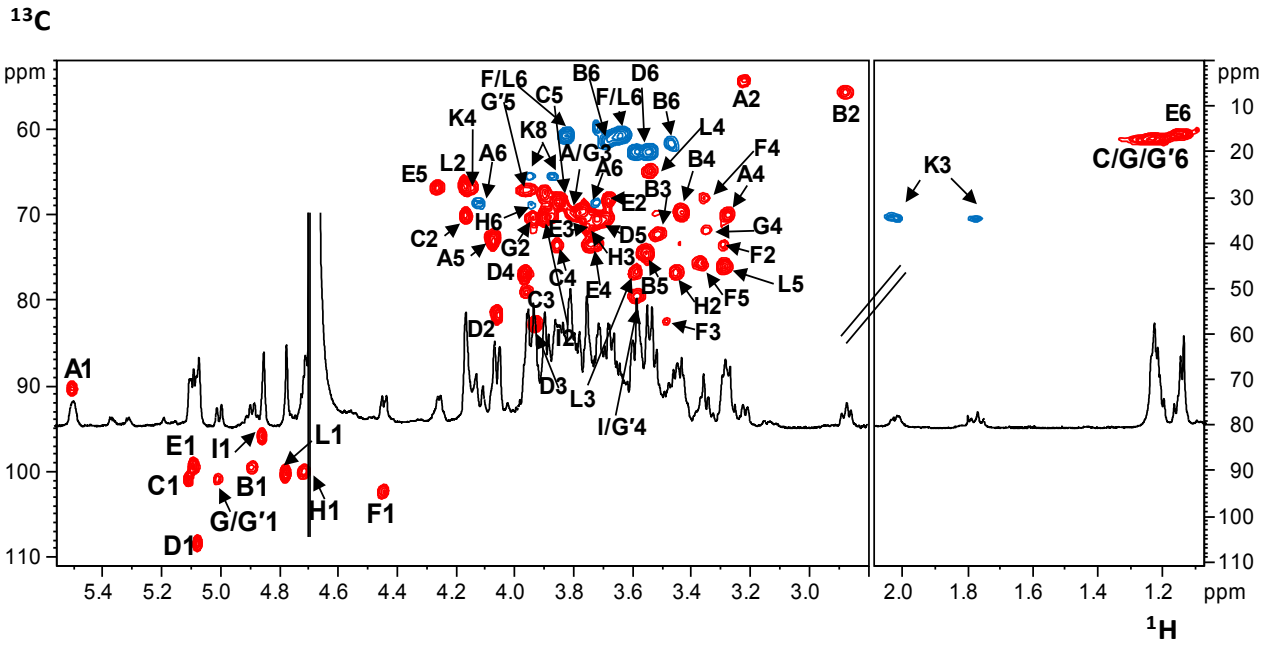

Figure S2. ^{1}H and ^{1}H, ^{13}C HSQC NMR spectrum of fully deacylated LPS_{Bv}. Key heteronuclear signals from the sugar backbone are indicated. Numbering of sugar residues is as reported in Table 1.

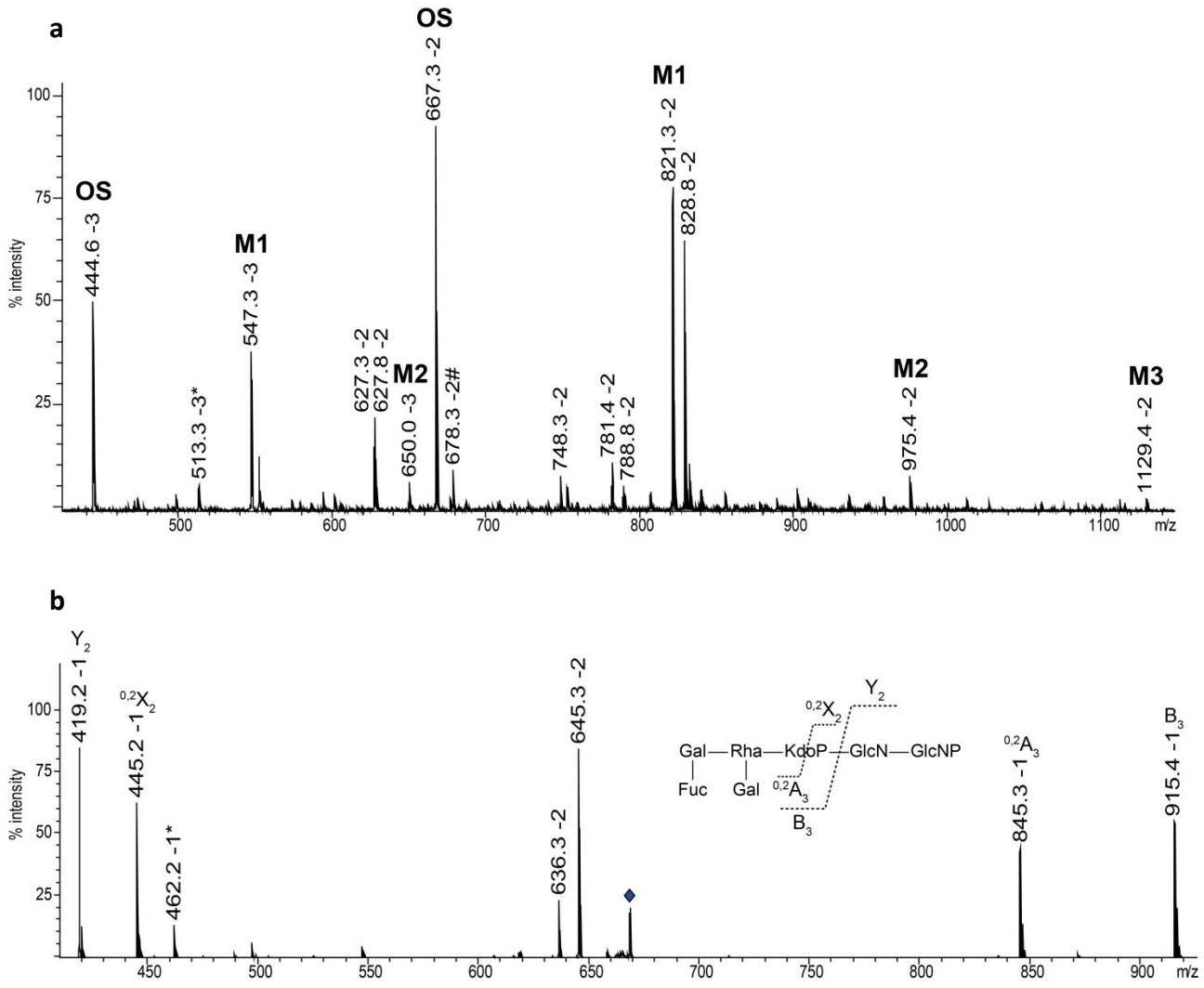

Figure S3. ESI-MS spectrum of fully deacylated LPS_{Bv} and ESI-MS^2 spectrum of core OS from LPS_{Bv}. (**a**) Zoom of mass spectrum with ions corresponding to core OS and core OS substituted with one, two and three O-chain repeating units (*m/z* 444.6 and 667.3 (OS), 547.3 and 821.3 (**M1**), 650.0 and 975.4 (**M2**), as well as 1129.4 (**M3**) respectively. # indicates $[M-3H+Na]^{2-}$ ion. Ion indicated by asterisk was not interpreted. (**b**) Core OS was selected for MS^2 fragmentation. B_3 and Y_2 ions are indicated. Other ions indicate fragmentation inside the sugar ring (A_3 and X_2) with loss of formyl group (*m/z* 645.3, 636.3 and X_2). The inset structure represents general structure of core OS. The precursor ion (*m/z* 667.3) is indicated by diamond. Ion indicated by asterisk was not interpreted.

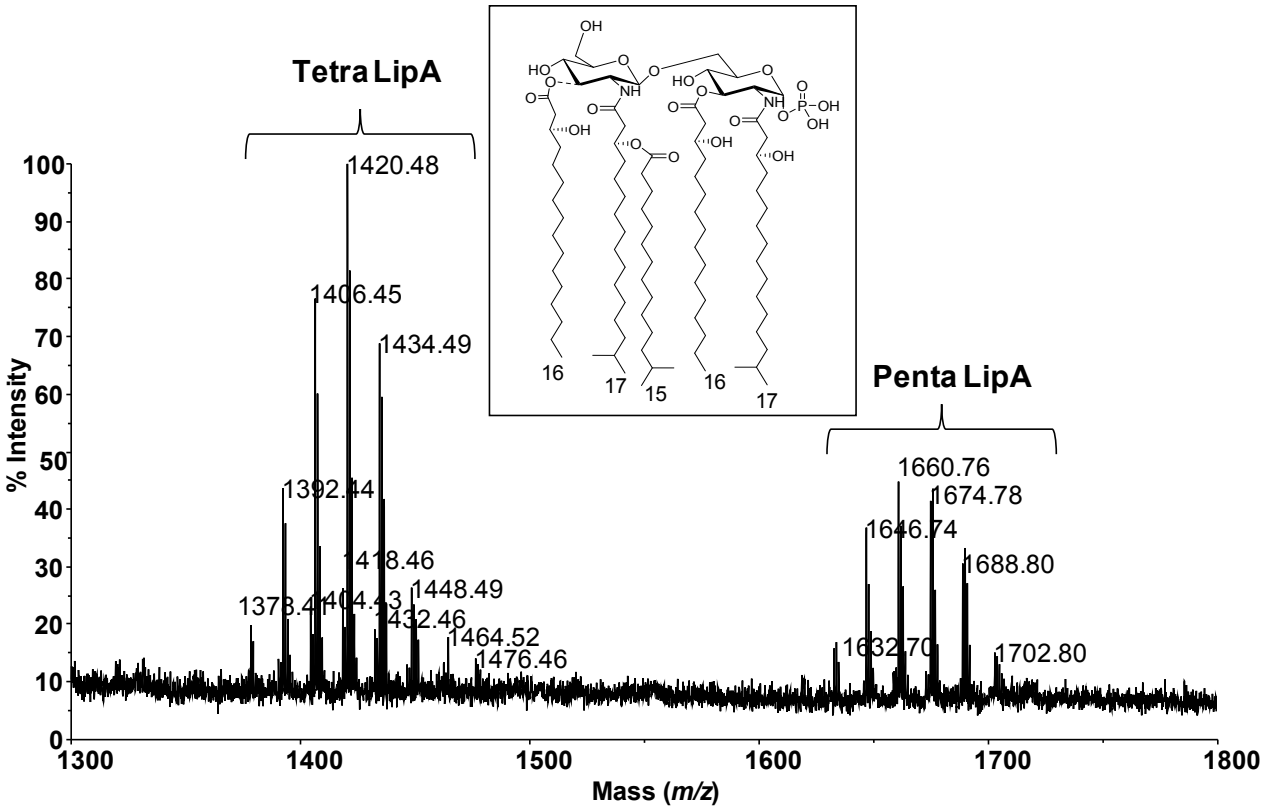

Figure S4. MALDI MS spectrum of *B. vulgatus* Lipid A. Zoom of reflectron MALDI TOF mass spectrum, acquired in negative polarity, of purified *B. vulgatus* mpk lipid A. Mass differences of 14 Da, indicative of lipid A species differing in their acyl chain length, are clearly visible. Assignment of the lipid A species is depicted as TetraLip A (tetra-acylated) and PentaLip A (penta-acylated). In the inset, structure of a representative *B. vulgatus* mpk lipid A species, relative to ion at *m/z* 1688.3 is depicted.

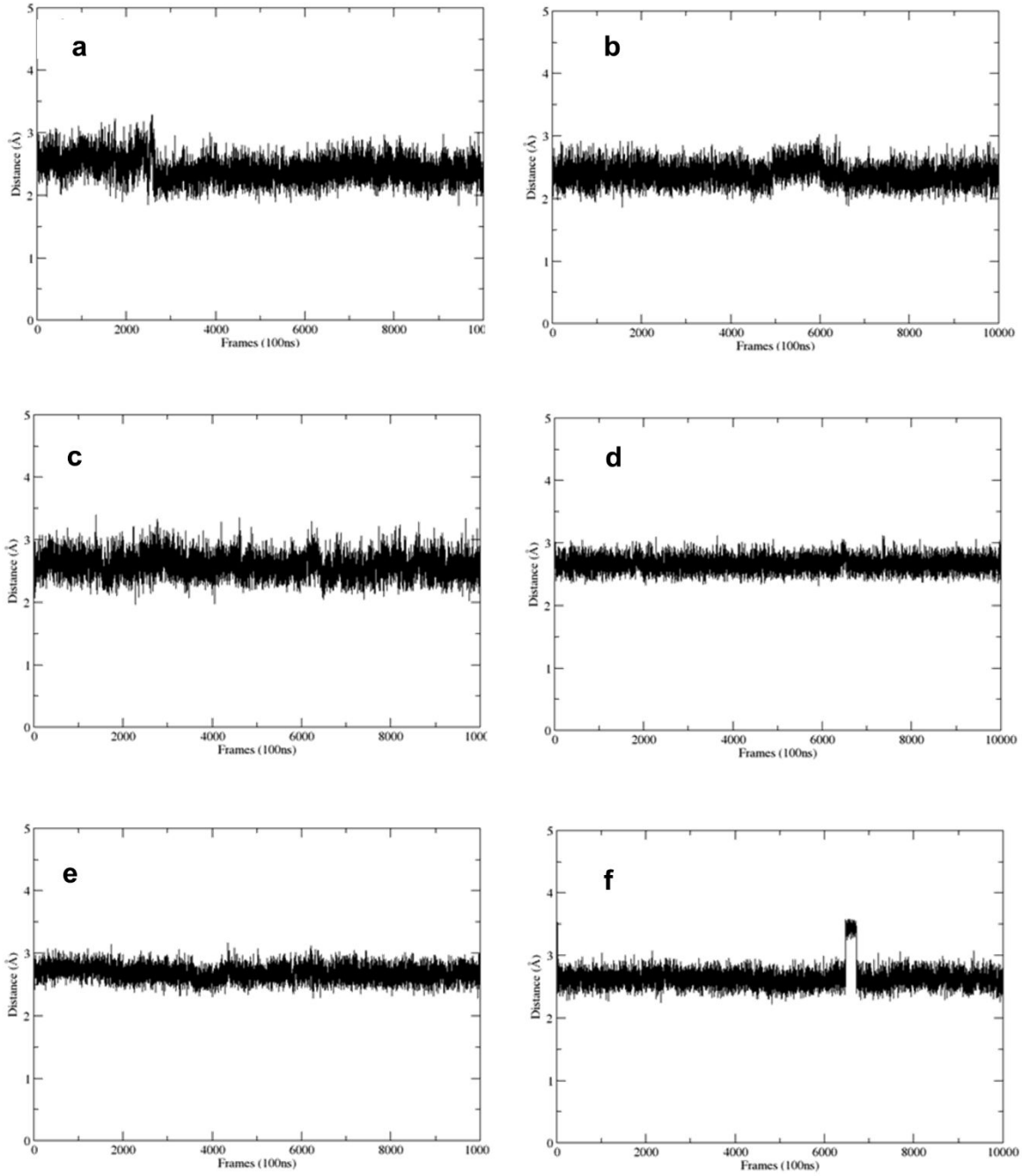

Figure S5. Inter-residue distances of tetra-acylated LPS_{Bv}. Distances in Angstroms between (**a**) H1 of **B** and H6 of **A**; (**b**) H1 of **D** and H3 of **C**; (**c**) H1 of **H** and H3 of **C**; (**d**) C2 of H and H1 of **E**; (**e**) C3 of **F** and H1 of **G**; (**f**) C6 of **H** and H1 of **F** during the 100ns MD simulation of tetra-acylated LPS_{Bv}.

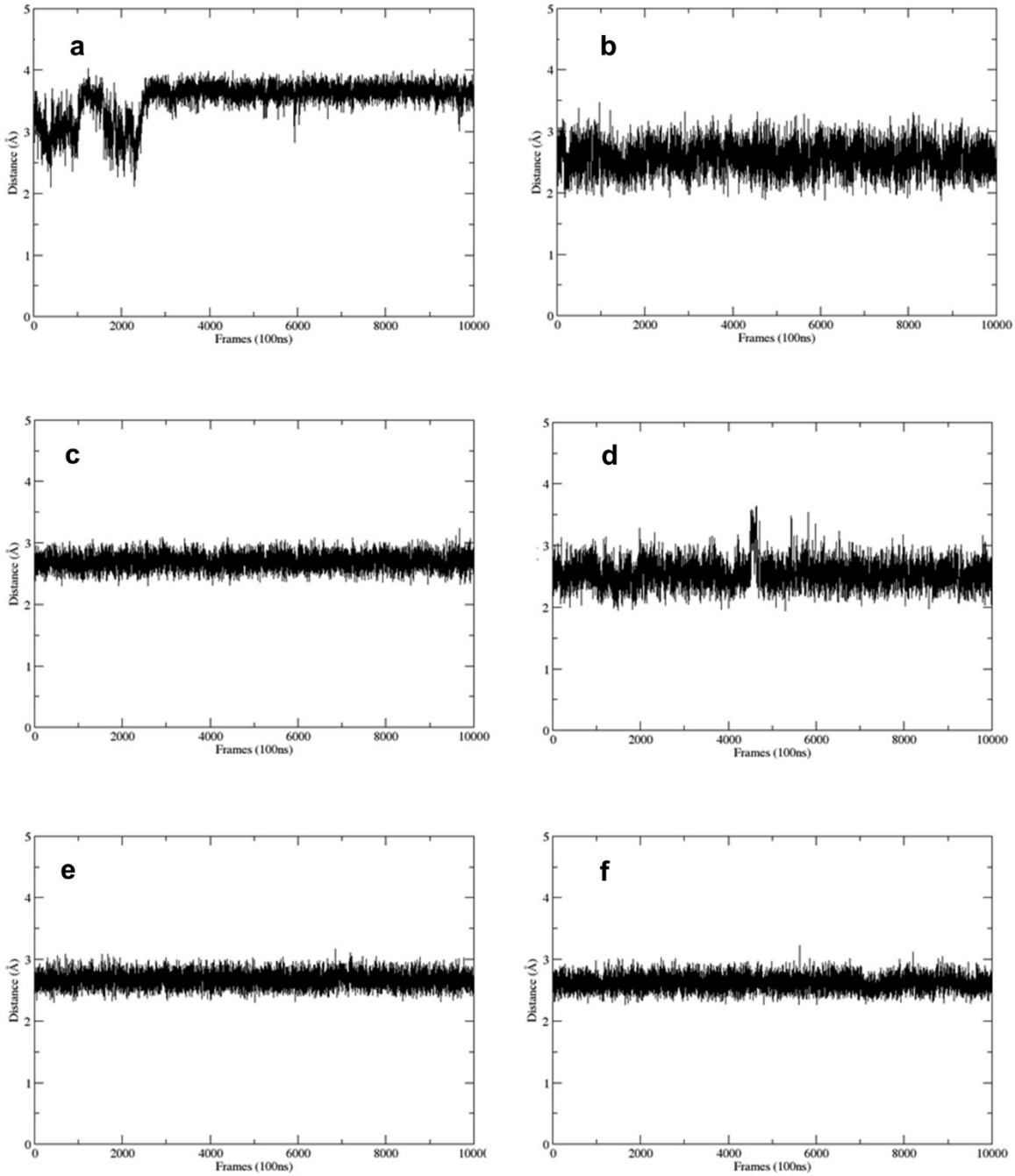

Figure S6. Inter-residue distances of penta-acylated LPS_{Bv}. Distances in Angstroms between (**a**) H1 of **B** and H6 of **A**; (**b**) H1 of **D** and H3 of **C**; (**c**) H1 of **H** and H3 of **C**; (**d**) C2 of **H** and H1 of **E**; (**e**) C3 of **F** and H1 of **G**; (**f**) C6 of **H** and H1 of **F** during the 100ns MD simulation of penta-acylated LPS_{Bv}.

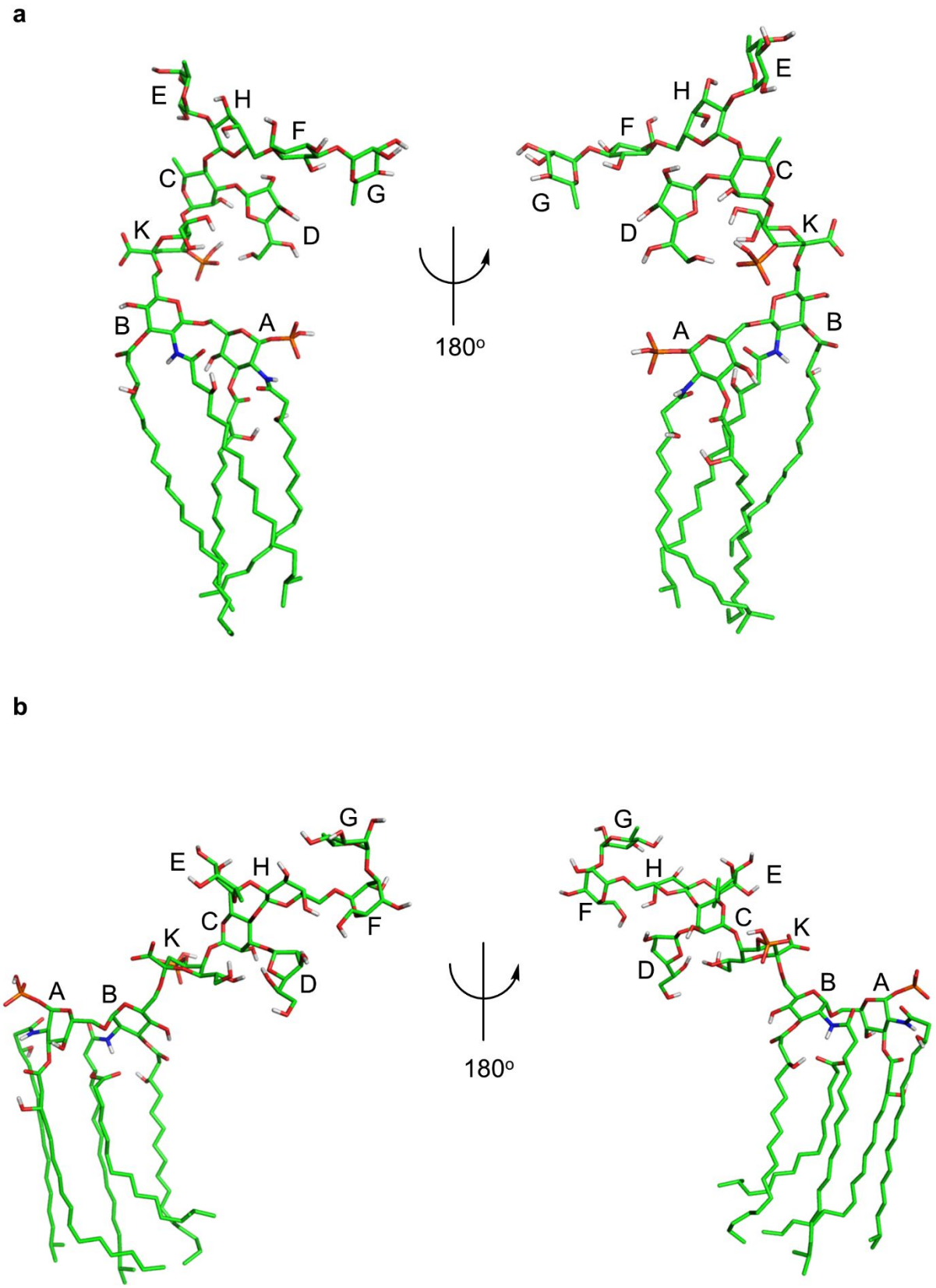

Figure S7. 3D structure of tetra-acylated (**a**) and penta-acylated (**b**) LPS_{Bv} from MD simulation in water. Monosaccharide units are depicted.

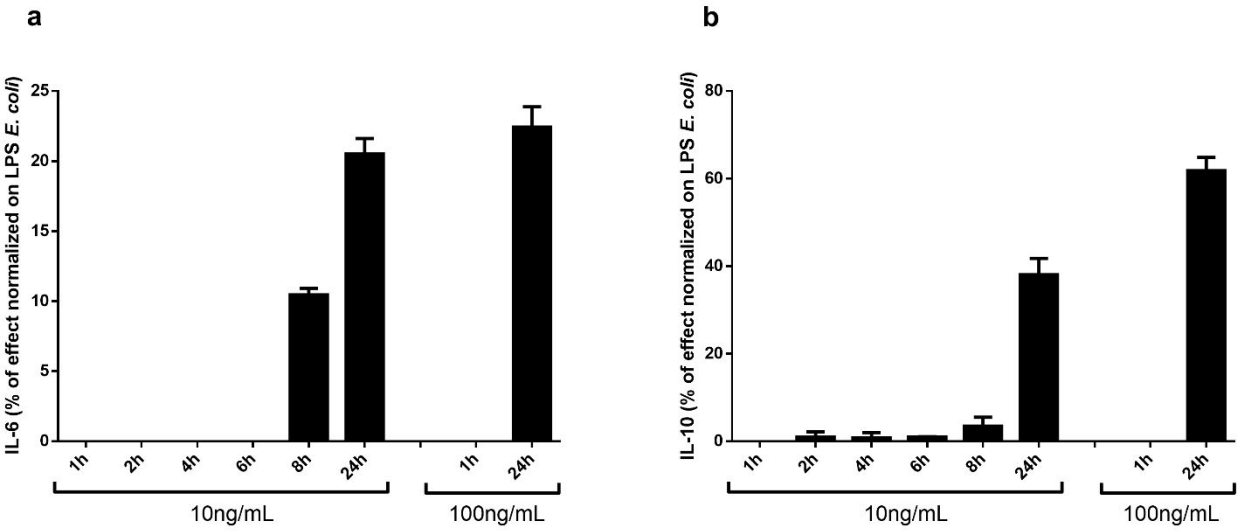

Figure S8. IL-6 (**a**) and IL-10 (**b**) release in Peripheral Blood-Monocyte-Derived Dendritic Cells (MoDCs) stimulated with LPS_{Bv} at different time points measured by ELISA. Data are expressed as percentage of effect and they are normalized over the MoDCs treated with *E. coli* LPS (10 ng/mL at 24 h) set at 100 %. The average results from two donors are shown. Error bars represent the standard deviation of the experiment performed in duplicate.

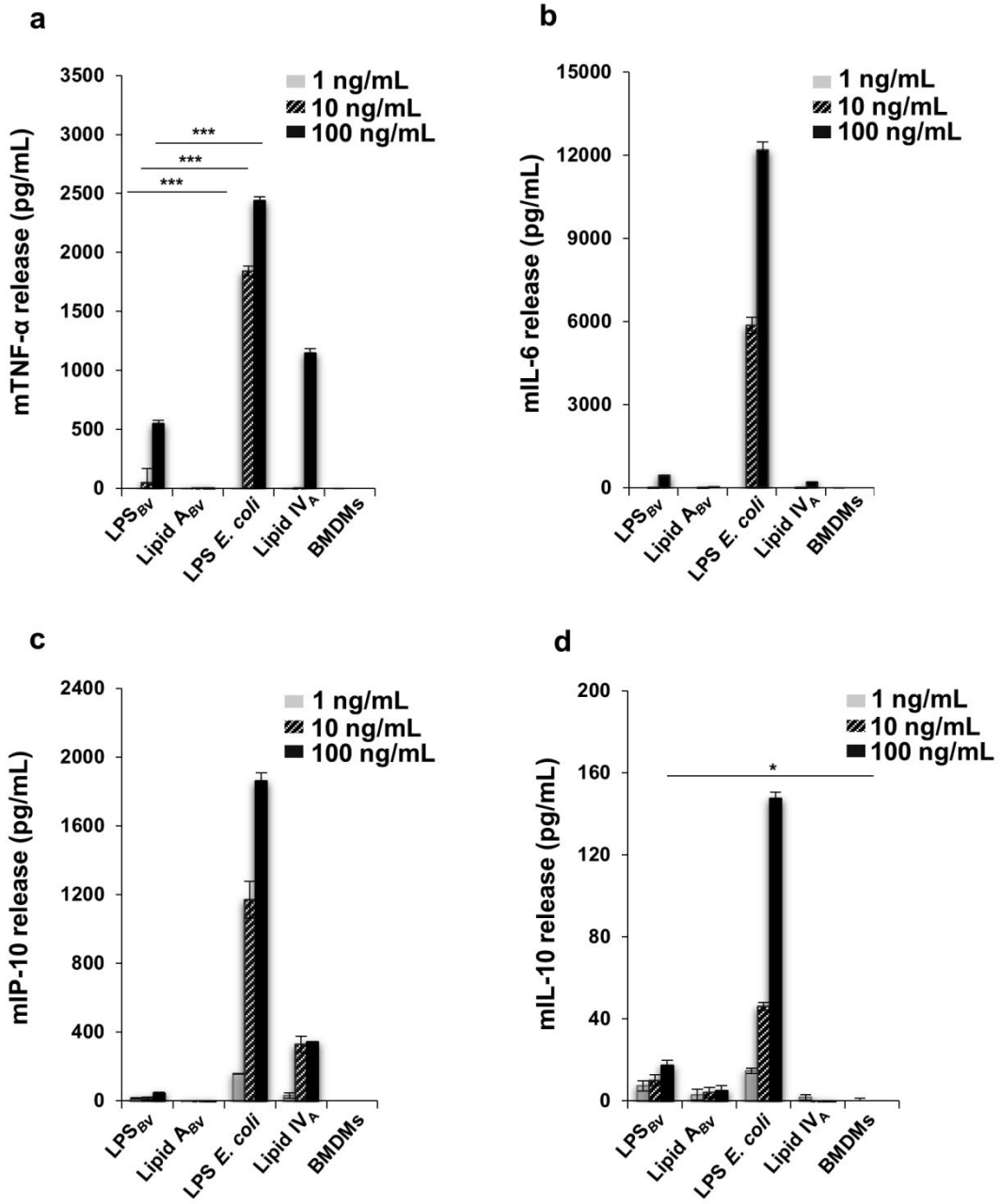

Figure S9. Cytokine and chemokine release induced by LPS_{Bv} and lipid A_{Bv} in murine Bone Marrow Monocyte-derived Macrophages (BMDMs). Release of Tumor Necrosis Factor-α (TNF-α) (**a**), IL-6 (**b**), IP-10 (**c**) AND IL-10 (**d**) in BMDMs free supernatants of BMDMs stimulated with LPS_{Bv} or lipid A_{Bv}, with *E. coli* LPS and with the synthetic antagonist tetra-acylated lipid IV_A at the concentration of 1, 10 and 100 ng/mL during 12 hours. Cytokine and chemokine release was analyzed through ELISA. Data are expressed as mean ± SD of four independent experiments in triplicate. Untreated cells are the negative control in this experiment. *p<0.05, **p<0.01, ***p<0.001.

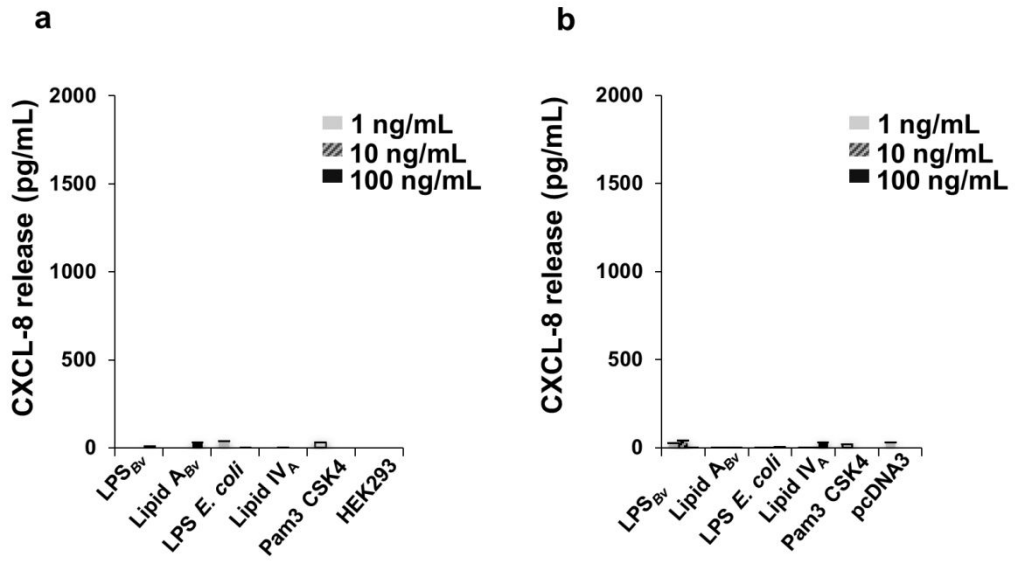

Figure S10. Analysis of immunopotential of LPS_{Bv} and Lipid A_{Bv} in HEK293 cells and HEK293 cells carrying pcDNA3. HEK293 cells (**a**) and HEK293 pcDNA3 (**b**) were treated for 6 hours with LPS_{Bv} or lipid A_{Bv}, with *E. coli* LPS or with the tetra-acylated lipid IV_A at the concentration of 1, 10 or 100 ng/mL, or with the synthetic TLR2 agonist Pam3 CSK4 (500 ng/mL) for 6 hours. After this time the release of the cytokine CXCL-8 was quantified through ELISA. Untreated cells were the negative control in these experiments.

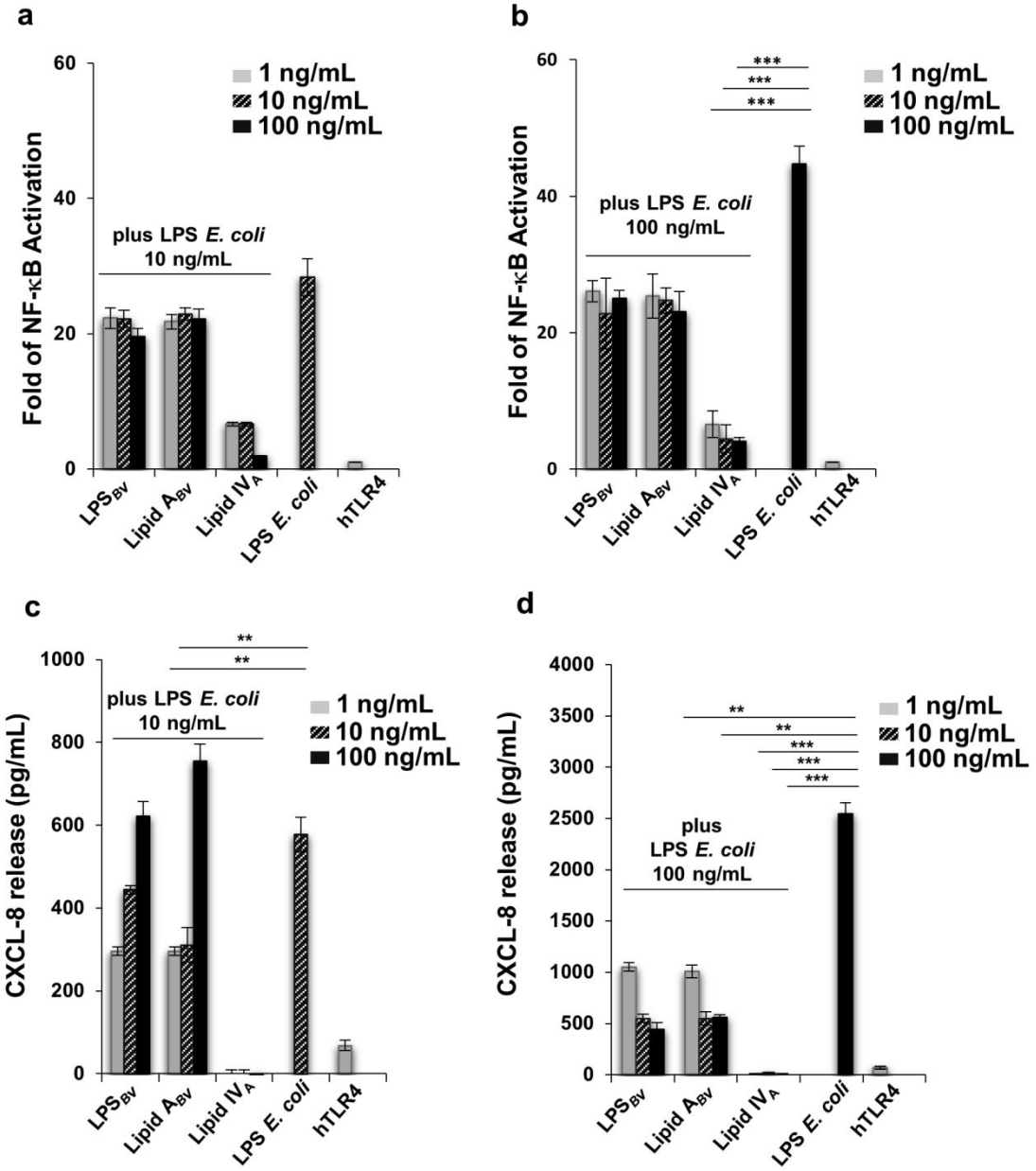

Figure S11. Competition assay between LPS_{Bv} or lipid A_{Bv} with *E. coli* LPS for hTLR4 binding. Fold of NF-κB activation (**a** and **b**) and CXCL-8 release (**c** and **d**) in HEK293 hTLR4/MD2-CD14 cells primed with LPS_{Bv} or lipid A_{Bv} or with lipid IV_A at the concentration of 1, 10 and 100 ng/mL for 1 hour and then stimulated with 10 (**a** and **c**) or 100 ng/mL (**b** and **d**) of *E. coli* LPS for 4 hours. Data are expressed as mean ± SD of four independent experiments in triplicate. Untreated cells are the negative control in these experiments. *p<0.05, **p<0.01, ***p<0.001.